

Magnetotransport in Transition Metal Multilayered Structures

S. S. P. Parkin

IBM Research Division, Almaden Research Center,
650 Harry Road, K11/D2, San Jose, CA 95120-6099, USA

Abstract

Metallic multilayered structures comprising alternating ferromagnetic and non-ferromagnetic layers exhibit enhanced magnetoresistance values compared with the magnetoresistance of the individual magnetic layers. The largest changes in resistance are found in sputter-deposited 110 oriented crystalline Co/Cu multilayers in which the Co layers are doped with small amounts of Fe. Values of *giant magnetoresistance* (GMR) of $\sim 110\%$ at room temperature and $\sim 220\%$ at 4.2 K are found. The origin of the magnetoresistance relates to spin-dependent scattering at the interfaces between the Co and Cu layers. These very large MR values make GMR materials attractive for a variety of applications for which magnetic field sensors are required. Simple exchange-biased sandwich structures (*spin-valve* sandwiches) are described which exhibit large changes in resistance in very small fields.

1 Introduction

In recent years there has been a great deal of interest in the magnetic and transport properties of metallic multilayered thin film structures composed of thin $3d$ transition metal ferromagnetic layers separated by thin non-ferromagnetic spacer layers. These systems display unique properties, notably an oscillatory indirect exchange coupling of the ferromagnetic (FM) layers via the non-ferromagnetic spacer layers, and enhanced magnetoresistance. The latter has come to be called *giant magnetoresistance* (GMR). In this brief report the properties of these systems are reviewed with an emphasis on recent results in sputtered crystalline multilayers containing copper spacer layers.

2 Giant magnetoresistance in polycrystalline Co/Cu multilayers

Typical 3d ferromagnetic metals or alloys display only small changes in their resistance when subjected to magnetic fields at room temperature (McGuire and Potter, 1975). Maximum magnetoresistance values of about 5–6% are found in Ni–Co and Ni–Fe alloys. In magnetic fields large enough to saturate the magnetic moment of such metals their resistance primarily depends on the orientation of their magnetic moment with regard to the direction of the sense current passing through the sample. Thus they display an *anisotropic* magnetoresistance (AMR) such that their resistance can be written as $\rho = \rho_0 + \Delta\rho \cos^2 \theta$, where θ is the angle between the magnetic moment of the sample and the direction of the current (McGuire and Potter, 1975; Rossiter, 1987). The resistance is typically higher when the magnetic moment of the sample is aligned orthogonal to the sense current. In magnetic fields not large enough to saturate the magnetization of the metal the resistance depends on the detailed magnetic domain structure. In thin ferromagnetic films the magnitude of the AMR effect becomes even smaller as the thickness of the FM layer is decreased because scattering of the conduction electrons from the outer boundaries of the film increases the resistance of the film. These scattering processes do not give rise to AMR.

The same AMR phenomenon is displayed by thin ferromagnetic layers in metallic multilayers but the magnitude of the effect is further reduced. By contrast certain magnetic multilayers, containing very thin ferromagnetic layers can display very large or *giant* changes in resistance with magnetic field of a different origin (Parkin, 1994; Fert and Bruno, 1994; Parkin, 1995; Levy, 1994). The largest GMR effects have been found in multilayers, prepared by sputter deposition, composed of alternating thin Co and thin Cu layers. In such polycrystalline Co/Cu multilayers GMR effects as large as 70–80% at room temperature have been reported (Parkin et al., 1991b). An example is shown in Fig. 1.

The origin of the giant magnetoresistive effect is quite different from that of AMR. GMR is found in multilayered and other inhomogeneous magnetic structures in which the magnetic layers [or other entities such as magnetic granules in magnetic granular metals (Chien, 1995)] are oriented non-parallel to one another for some range of magnetic field, and, such that, with application of a sufficiently large magnetic field, the magnetic moments of the layers (or entities) become oriented parallel to one another. It is the change in the magnetic configuration which affects the scattering of the conduction electrons propagating between the magnetic layers or entities and which thereby gives rise to GMR. In Co/Cu multilayers, for certain thicknesses of Cu, the moments of the Co layers are arranged antiparallel to one

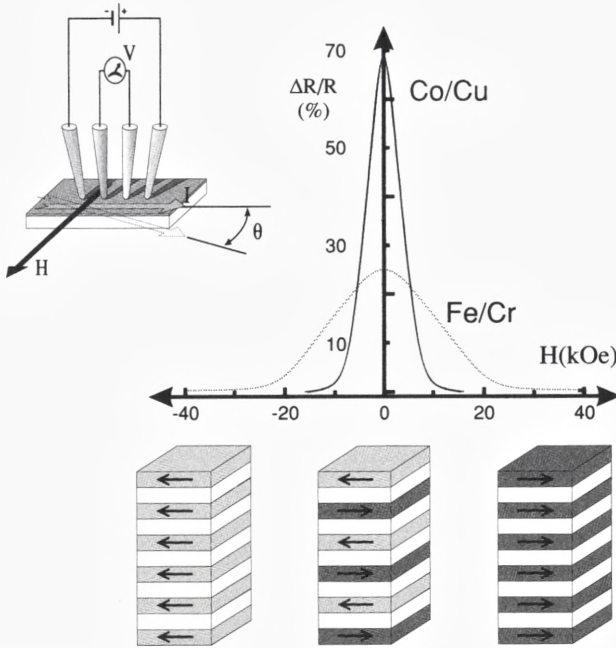


Figure 1. Resistance versus in-plane magnetic field curve for a polycrystalline Co/Cu multilayer exhibiting nearly 70% change in resistance at room temperature (Parkin et al, 1991b). The measurement geometry is shown in the top left corner. A schematic diagram of the Co/Cu layer is shown for large negative, zero and large positive fields.

another in small fields because of an antiferromagnetic (AF) coupling of the Co layers mediated via the Cu spacer layers. When a magnetic field is applied, large enough to overcome the AF interlayer coupling, the Co moments become aligned parallel to each other and to the applied field. This is shown schematically in Fig. 1.

Polycrystalline Co/Cu multilayers are usually (111) textured for thin Co and Cu layers, although the texture changes to (100) for thick Cu layers (Parkin et al., 1993), or when the multilayer is grown on thick Cu buffer layers (Lenczowski et al., 1994). Polycrystalline multilayers usually display little in-plane magnetic anisotropy. Consequently the resistance of such multilayers typically varies continuously with magnetic field independent of the orientation of the magnetic field in the plane of the sample (Parkin et al., 1990, 1991b,c). For strongly antiferromagnetically coupled multilayers, as the magnetic field is increased, the angle between neighbouring magnetic layers, $\sim 180^\circ$ in small fields, smoothly decreases

until at magnetic fields large enough to overcome the antiferromagnetic interlayer exchange coupling the magnetic moments become aligned parallel to the magnetic field and to each other. When multilayers are crystalline and have significant magnetic anisotropy the dependence of resistance on magnetic field is more interesting and can display quite unusual behaviour as discussed in Sect. 3.

As shown in Fig. 2 the magnitude of the giant magnetoresistance effect oscillates as a function of copper thickness. The oscillation in saturation magnetoresistance

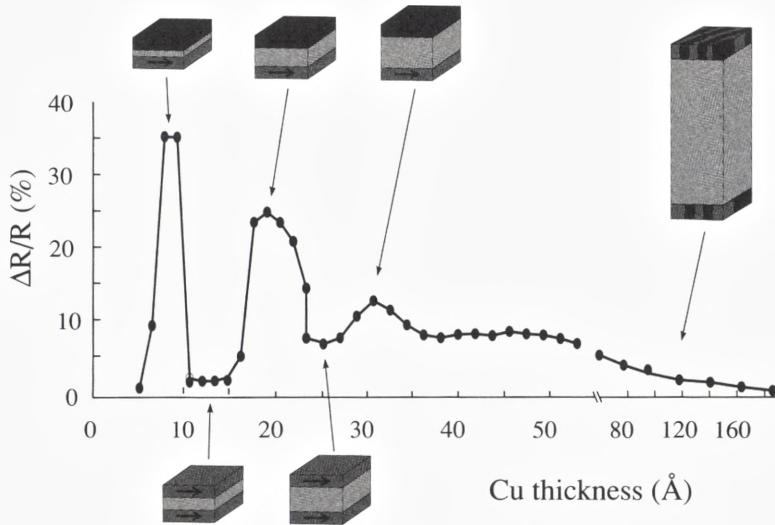


Figure 2. Room temperature saturation magnetoresistance versus Cu spacer layer thickness for a series of Co/Cu multilayers (Parkin et al, 1991a). The magnetic state of the multilayers are shown schematically for various Cu spacer layer thicknesses (only two Co layers are shown).

is related to an oscillation in the interlayer coupling between antiferromagnetic (AF) coupling and ferromagnetic (F) coupling as the Cu spacer thickness is varied. This is shown schematically in Fig. 2. Similar oscillations in magnetoresistance and interlayer coupling were first observed in Fe/Cr and Co/Ru multilayers (Parkin et al., 1990).

The coupling via Cu, Cr, Ru and other transition and noble metals is long-range and of the RKKY type. In polycrystalline Co/Cu multilayers the oscillation period is ~ 10 Å. The first observation of oscillatory interlayer coupling in transition

metal multilayers was in Fe/Cr and Co/Ru sputtered polycrystalline multilayers (Parkin, 1994). Subsequently it was shown that oscillatory interlayer coupling is exhibited by nearly all of the $3d$, $4d$, and $5d$ non-ferromagnetic transition and noble metals (Parkin, 1991). Later oscillatory coupling was observed in single-crystalline Fe/Cr and Co/Cu films grown by evaporation techniques in ultra-high vacuum chambers (Pierce et al., 1994; Johnson et al., 1992). For (100) Fe/Cr and (100) Co/Cu the interlayer exchange coupling oscillates with Cr and Cu spacer layers with two superposed oscillation periods, one long and one short (Unguris et al., 1991; Weber et al., 1995). For Fe/Cr the short period corresponds remarkably to just 2 monolayers of Cr (Unguris et al., 1991; Rührig et al., 1991). The magnitude of the oscillation periods for noble metal spacer layers can be well accounted for by examination of the Fermi surfaces of the noble metals. The oscillation periods are related to wave-vectors which span or nest the Fermi surface (Bruno and Chappert, 1992; Mathon et al., 1995).

3 Giant magnetoresistance in [110] crystalline Co/Cu and Co-Fe/Cu multilayers

3.1 Structure

There has been a great deal of work in the past few years to optimize the magnitude of the magnetoresistance in magnetic multilayers but especially Co/Cu and related systems because Co/Cu exhibits the largest GMR effects at room temperature. The magnitude of the GMR is increased with increasing number of Co/Cu bilayers and for very thin Co and Cu layers (the Cu thickness has to be one which gives rise to well defined anti-parallel orientation of the Co layers). Figure 3 shows a plot of resistance versus magnetic field for a Co-Fe/Cu multilayer displaying by far the highest GMR yet found. The film displays a value of room temperature magnetoresistance (MR) of $\Delta R/R_s \sim 110\%$, where R_s is the saturation resistance in large fields. At 4.2K the MR is even higher $\Delta R/R_s \sim 220\%$. The Co-Fe/Cu sample in Fig. 3 is composed of 120 bilayers of $[9.5\text{\AA} \text{Co}_{95}\text{Fe}_5 / 8.5\text{\AA} \text{Cu}]$ grown by seeded epitaxy (Farrow et al., 1993; Harp and Parkin, 1994, 1996) on a MgO(110) single crystal substrate. Seed layers of $6\text{\AA} \text{Fe} / 45\text{\AA} \text{Pt}$ are first deposited at $\sim 450^\circ\text{C}$. The $\text{Co}_{95}\text{Fe}_5/\text{Cu}$ multilayer is grown after cooling the substrate to $\sim 40^\circ\text{C}$ to reduce interdiffusion of the metal layers. Specular x-ray diffraction and cross-section transmission electron microscopy (XTEM) characterization of the structure of the multilayer show that the Fe/Pt seed layers and the multilayer grow highly oriented with respect to the substrate crystallographic axes. By using (100) oriented MgO and (0001) Al_2O_3 substrates, (100) and (111) oriented fcc Co/Cu and Co-Fe/Cu

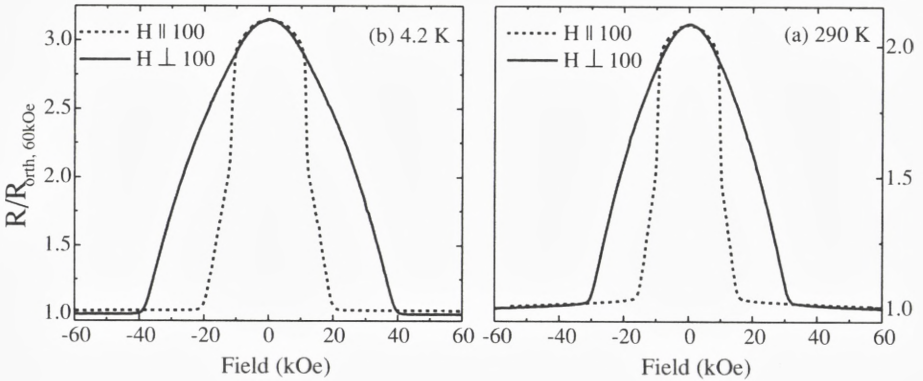


Figure 3. Resistance versus field curves at (b) 4.2 K and (a) 290 K of a magnetic multilayer of the form MgO(110)/ 6Å Fe/ 45Å Pt/ 9.5Å Cu/ [9.5Å Co₉₅Fe₅/ 8.5Å Cu]₁₂₀/ 12Å Pt. Curves are shown for the magnetic field applied in the plane of the film parallel and perpendicular to [100]. The current is applied along the [100] direction.

multilayers can be grown. Identical (100), (110) and (111) Co(Fe)/Cu multilayered structures can be prepared by simultaneous deposition onto these various MgO and sapphire substrates (Smith et al., 1997).

The structure of representative Co/Cu multilayers (grown without Fe seed layers) was characterized in detail with specular and off-specular x-ray scattering measurements using wiggler beam line VII-2 at the Stanford Synchrotron Radiation Laboratory (Smith et al., 1997). The weak scattering contrast between Co and Cu was enhanced by utilizing the Co scattering factor resonant modification obtained for 7692 eV photons close to the 7709 eV Co K absorption edge. Modeling of low angle specular scattering data, using an optical recursion formulation of the reflectivity (Parratt, 1954; Toney and Thompson, 1990), revealed that the Co/Cu interfaces had a typical root mean square width of ~ 4.5 Å where the averaging is over the spectrometer in-plane coherence length (~ 5000 Å). Peaks in the slightly off-specular diffuse scattering at the multilayer periodicity demonstrate that significant long wavelength interfacial roughness is conformally replicated throughout the multilayer (Sinha et al., 1991; Lurio et al., 1992).

The epitaxy, mosaicity and structural coherence of various Co/Cu films was explored by large-angle Bragg scattering. Figure 4 shows azimuthal x-ray scans (rotation about the multilayer normal) through off-specular Bragg peaks for three Co/Cu multilayers, which demonstrate both the symmetry of the films and the excellent in-plane orientational order with respect to the substrate crystallographic axes. Whilst orientationally ordered, the films are not strictly epitaxial as the

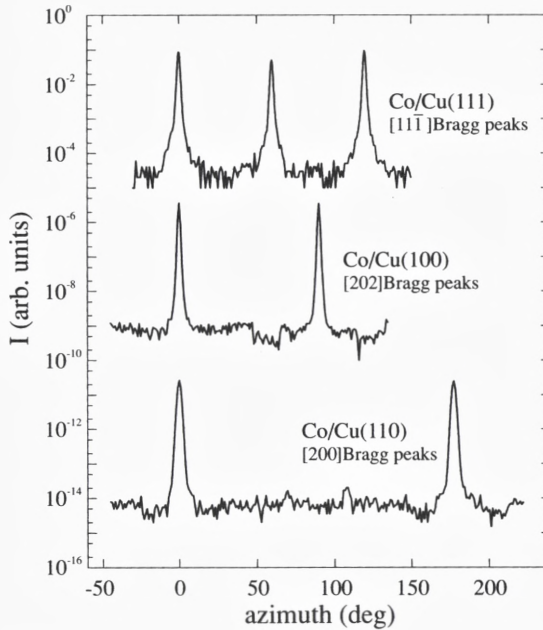


Figure 4. Azimuthal scans through off-specular Bragg peaks: six-fold symmetric (twinned three-fold) $[11\bar{1}]$ peaks from a $\text{Co}[10\text{\AA}]/\text{Cu}[9\text{\AA}]$ (111) oriented film, four-fold symmetric $[202]$ peaks from a $\text{Co}[20\text{\AA}]/\text{Cu}[20\text{\AA}]$ (100) oriented film, and two-fold symmetric $[200]$ peaks from a $\text{Co}[10\text{\AA}]/\text{Cu}[9\text{\AA}]$ (110) oriented film. Successive scans are scaled by 10^{-5} .

Co/Cu lattices are relaxed relative to that of the underlying seed film, although the largest observed Co/Cu in-plane strain relative to the bulk metals is $< 0.2\%$. Note that when the very thin Fe seed layer is omitted, for growth on (100) and (110) MgO , the Pt seed layer, and consequently the multilayer, may grow with mixed orientations, and typically some (111) orientation is then obtained. Interestingly, the (111) phase grows oriented with respect to the substrate crystal axes. The Co/Cu films exhibit modest structural coherence lengths as summarized in Table I for four representative films. Although the data in Table I correspond to Co/Cu multilayers grown without Fe seed layers, of the films examined, only one grew with mixed orientation.

Figure 5(a) shows a high resolution XTEM image of a (100) Co/Cu multilayer grown on $\text{MgO}(100)$ with an Fe/Pt seed layer. The sample was prepared for electron microscopy using standard procedures of mechanical polishing and dimpling, followed by Ar^+ ion milling at 77 K. The microscopy was carried out using a JEM-

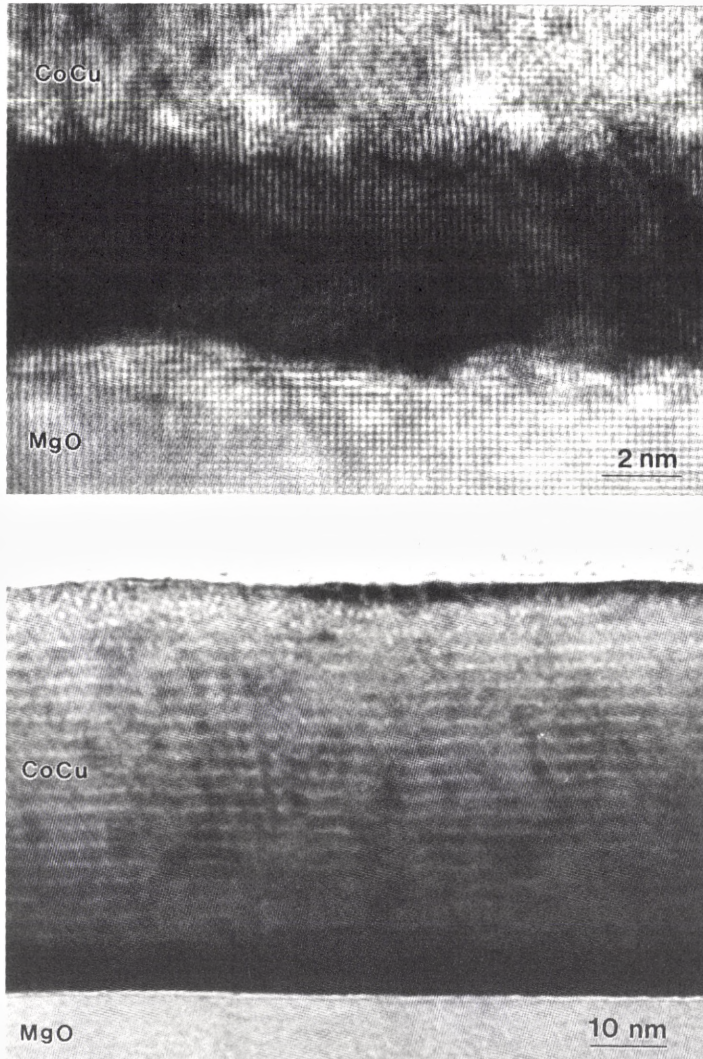


Figure 5. (a) High-resolution cross-section transmission electron micrograph of a MgO(100)/ 5 Å Fe/ 50 Å Pt/[11 Å Co/ 13 Å Cu]₁₉/ 11 Å Co/ 15 Å Pt multilayer. (b) Low magnification electron micrograph showing cross-section of the same multilayered structure as in Fig. 3(a) but deposited on a MgO(100) substrate. The image is deliberately defocused to enhanced layer contrast. A section of the structure including, MgO substrate, Fe/Pt seed layer and a lower portion of the multilayer is shown.

Table I. Structural characteristics of four representative multilayers. Only one sample displayed mixed orientation. Tabulated mosaics are multilayer normal (\perp) or in-plane (\parallel) Bragg peak rocking full widths at half maximum. Coherence lengths (ξ_{\perp} , ξ_{\parallel}) are resolution corrected Bragg peak inverse half widths at half maximum.

Substrate	Orientation	Mosaic $_{\perp}$ (Deg.)	ξ_{\perp} (Å)	Mosaic $_{\parallel}$ (Deg.)	ξ_{\parallel} (Å)
Al ₂ O ₃ (0001)	111	1.1	227	1.5	37
MgO (110)	110	1.4	61	1.2	47
MgO (100)	100	1.0	96	0.8	89
MgO (110)	100	2.2	41	1.6	42
MgO (110)	111	0.7	184	2.0	44

4000EX high-resolution electron microscope operated at 400 keV. The micrograph shows that the Pt seed layer and Co/Cu are epitaxially oriented with the MgO(100) substrate, and that the multilayer is of high crystalline quality with few defects. Under optimum imaging conditions the Co and Cu layers cannot be distinguished. However by deliberately defocussing the image the contrast between the Co and Cu layers is enhanced (Smith et al., 1994). Fig. 5(b) shows an XTEM of exactly the same multilayered structure as in Fig. 5(a) but grown, at the same time, on a MgO(110) substrate. The low resolution image shows that the Co and Cu layers are well defined and essentially flat. High resolution microscopy of the same sample shows that the crystal perfection is not as great as for the (100) oriented multilayer but that there are a substantial number of stacking faults along the $\langle 111 \rangle$ planes.

3.2 Magnetic properties: bilinear and biquadratic interlayer coupling

For crystalline multilayers with significant in-plane magnetic anisotropy the resistance varies in a complicated manner with magnetic field as first observed in (100) Fe/Cr/Fe sandwiches (Binasch et al., 1989). The magnetic properties of (100) and (211) Fe/Cr multilayers, which exhibit a two-fold (uniaxial) and a four-fold magnetic anisotropy respectively, have been examined in great detail (Fullerton et al., 1993, 1995; Azevedo et al., 1996). The magnetic moment versus field hysteresis loops of multilayers with different crystalline symmetries (and thus possessing two-fold, four-fold or higher-order magnetic anisotropies) and both bilinear and biquadratic interlayer coupling of adjacent magnetic layers has been extensively modeled (Folkerts, 1991; Dieny et al., 1990; Fujiwara, 1995; Almeida and Mills, 1995). The bilinear interlayer coupling varies as $\cos \theta$ where θ is the angle between the magnetic moments of adjacent magnetic layers, and favours parallel or antipar-

allel alignment of the magnetic moments. By contrast, the biquadratic interlayer coupling varies as $\cos^2 \theta$, thereby favouring perpendicular orientation of neighbouring magnetic moments. The bilinear coupling can be understood in terms of RKKY models but the biquadratic coupling strength (which similarly oscillates with spacer layer thickness) is too large to be accounted for within conventional models. A variety of models have been proposed to account for biquadratic coupling (Slonczewski, 1995). These are generally based on competition between competing ferromagnetic and antiferromagnetic interlayer interactions resulting, for example, from variations in individual layer thicknesses on the atomic length scale. For Fe/Cr, as mentioned above, the interlayer coupling oscillates with a period of just 2 monolayers of Cr which means the sign of the coupling can change from F to AF when the thickness of Cr is increased or decreased by just one atomic monolayer. Other models propose a competing interaction between an RKKY AF coupling and a F coupling derived from pinholes or perhaps significant local thickness variations in the spacer layer which lead to F coupling (Fulghum and Camley, 1995). For Fe/Cr the spin density wave in the Cr layers themselves has been invoked in yet another model (Slonczewski, 1995).

The dependence of the magnetic moment with magnetic field of the (110) Co/Fe/Cu sample shown in Fig. 3 is exhibited in Fig. 6 for a field oriented in-plane along (100). This sample exhibits a significant two-fold in-plane magnetic anisotropy as shown by the strong orientation dependence of the resistance versus in-plane magnetic field curves shown in Fig. 3. The field required to saturate the resistance is smallest when the field is applied parallel to $\langle 100 \rangle$ and largest when applied perpendicular to $\langle 100 \rangle$ along $\langle 011 \rangle$. The energy, E_i , of the i th magnetic layer in the multilayer per unit area can be written as

$$E = -\frac{1}{2} \left[J_1^{i,i+1} \cos \theta^{i,i+1} + J_1^{i,i-1} \cos \theta^{i,i-1} \right] + K_u \sin^2 \theta \quad (1)$$

where $\theta^{i,i\pm 1}$ is the angle between the i th magnetic moment and the two neighbouring magnetic moments, and θ is the angle between the applied magnetic field and the easy magnetic anisotropy axis. J_1 and K_u are the bilinear interlayer exchange coupling, and the uniaxial magnetic anisotropy energies respectively. The relative strengths of these energies can be determined from the magnetic fields required to saturate the magnetization of the multilayer along the magnetic easy and hard axes. From Fig. 3 it is readily deduced that K_u is large and is about 1/3 the size of J_1 .

The data in Fig. 6 show that there are two distinct field regions of magnetization for the (110) CoFe/Cu multilayer. At low fields the moment of the multilayer is close to zero consistent with the magnetic moments of adjacent layers being coupled antiferromagnetically (Cebollada et al., 1989; Parkin et al., 1991a). The

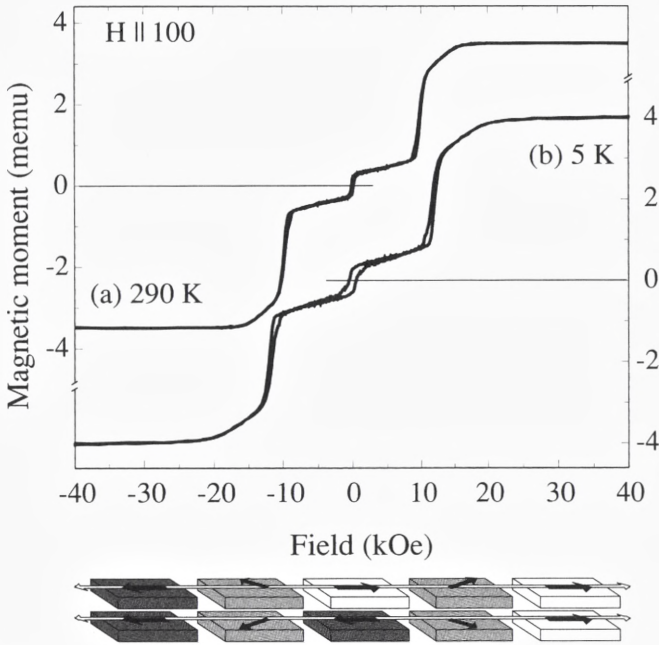


Figure 6. Magnetic moment versus field curves at (a) 300 K and (b) 5 K of a magnetic multilayer of the form MgO(110)/ 6Å Fe/ 45Å Pt/ 9.5Å Cu/[9.5Å Co₉₅Fe₅/ 8.5Å Cu]₁₂₀/ 12Å Pt for magnetic field applied in the plane of the film parallel to [100].

small residual moment may indicate that some small portion of the Co layers are coupled ferromagnetically, perhaps because of defects in the multilayer, or because of a small biquadratic interlayer coupling contribution. As the field is increased the moment of the multilayer increases slowly until at about 10 kOe the moment increases abruptly. The system undergoes a spin-flop transition at this field in which the moments reorient themselves from being aligned largely along $\langle 100 \rangle$ and antiparallel to one another to being aligned largely parallel to the applied field and each other (see sketch of magnetic configurations in Fig. 6). The sudden decrease in the angle between neighbouring moments results in a significant decrease in the resistance of the multilayer (see Fig. 3). For field oriented along the $\langle 110 \rangle$ in-plane axis, the magnetic hard axis, both the magnetization (not shown) and resistance (Fig. 3) vary monotonically with magnetic field. Similar results have been obtained for (211) Fe/Cr multilayers (Fullerton et al., 1993).

Figure 7 shows an unusual example of the magnetoresistance curve of a (110) MgO/ 9Å Fe/ 50Å Pt/ 10Å Cu/[8.5Å Co₈₅Fe₁₅/ 12Å Cu]₄₀ multilayer. In this

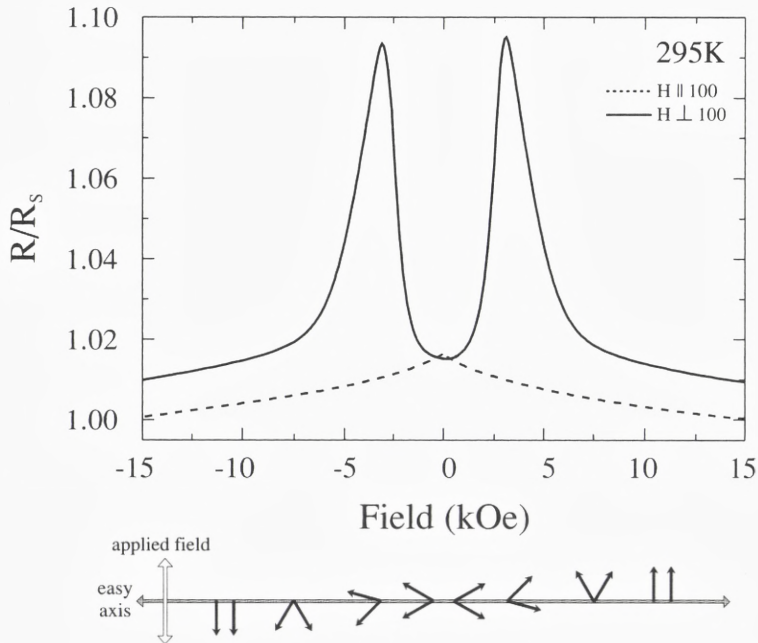


Figure 7. Resistance curve of a (110) MgO/ 9Å Fe/ 50Å Pt/ 10Å Cu/[8.5Å Co₈₅Fe₁₅/ 12Å Cu]₄₀ multilayer for field applied along the easy and hard in-plane axes.

case the resistance varies little when the magnetic field is applied along the easy axis (100) but when the field is applied along the hard axis the resistance, which is low in small fields, exhibits two peaks at fields of $\sim \pm 4$ kOe. This behaviour can only be accounted for by including a biquadratic interlayer exchange coupling contribution in addition to a ferromagnetic bilinear term and a uniaxial magnetic anisotropy (Pettit et al., 1997).

4 Giant magnetoresistance in sandwiches

The phenomena of giant magnetoresistance and oscillatory interlayer coupling have captured much attention, not only because they allow the basic transport and electronic properties of transition metals to be probed in a novel manner, but because it was immediately recognized that they may have useful properties for certain applications. In particular magnetoresistive materials can be used to measure magnetic fields. An important application is in magnetic recording disk drives in which in-

formation is stored in the form of magnetic bits written in thin magnetic films deposited on circular platters or discs. Bits correspond to small longitudinally magnetized regions or, rather, transitions between regions magnetized in opposite directions. An important parameter describing the performance of a disk drive is the number of magnetic bits which can be stored in a given area. In modern disk drives areal densities are in excess of 1 Gbit/in². In recent years the areal density has been increasing at a compound growth rate of approximately 60%/year (Grochowski and Thompson, 1994). This is reflected in decreased magnetic bit sizes which makes them increasingly difficult to read (as well as write). The most advanced magnetic recording read heads today use magnetoresistive technology based on the AMR effect in thin permalloy (Ni₈₁Fe₁₉) films (Ciureanu, 1992; Tsang et al., 1990). In order to achieve higher areal densities the thickness of the AMR sense film has to be decreased from approximately 150 Å at 1 Gbit/in² to well below ~100 Å at densities of > 5 Gbit/in². As mentioned previously the AMR effect is decreased in thin ferromagnetic films such that it is predicted that within the near future AMR metals will no longer provide sufficient signal for MR read head devices. Thus new materials are needed to allow ever greater areal densities in magnetic recording disk drives. Novel spin-valve sensors based on the GMR in magnetic sandwiches have been proposed (Dieny et al., 1991).

The spin-valve device is composed of two thin ferromagnetic layers separated by a thin Cu layer. The device relies on the exchange-biasing of one of the ferromagnetic layers to magnetically pin this layer. This effect, of ancient origin, is described schematically in Fig. 8. The magnetic hysteresis loop of a ferromagnetic layer is centered symmetrically about zero field. However certain combinations of thin ferromagnetic and antiferromagnetic layers display hysteresis loops which are displaced from zero field by an *exchange bias field* (Yelon, 1971). The origin of the effect is related to an interfacial exchange interaction between the AF and F layers and the fact that the magnetic lattice of the AF layer is essentially rigid, and little perturbed by even large external magnetic fields. Assuming the simplest possible AF structure of successive ferromagnetically ordered atomic layers whose moments alternate in direction from one layer to the next, one can readily appreciate that the uncompensated magnetic moment in the outermost AF layer at the AF/F interface will give rise to a exchange field which the F layer is subjected to. A long standing puzzle is why any exchange bias field is observed at all since one supposes that the interface between the F and AF layers is rough on an atomic scale (Malozemoff, 1988). As shown in Fig. 8, if the interface consists of atomic terraces whose length is less than the exchange length in the F metal there will be no net exchange anisotropy field. Note that similarly, if the AF layer is composed of randomly oriented magnetic domains, then this alone would quench the exchange bias field. In order to establish an exchange bias field the AF layer is usually de-

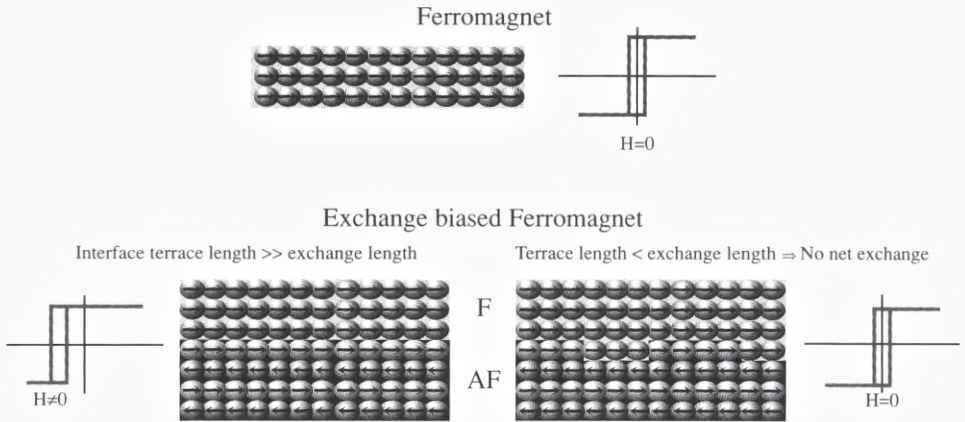
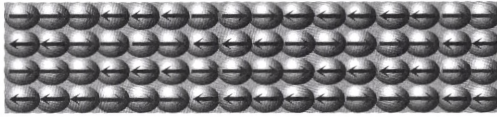


Figure 8. Schematic depiction of exchange biasing of a ferromagnetic layer by an antiferromagnetic layer on cooling through the blocking temperature of the AF layer.

posited on a magnetized F layer such that the interfacial exchange anisotropy leads to a preponderance of domains in the AF layer contributing to a net exchange bias field. Alternatively by heating the F/AF combination above the so-called blocking temperature of the AF layer where the AF spin system is no longer rigid, and subsequently cooling the bilayer couple in a magnetic field, an exchange bias field can be established in the direction of the applied field (see Fig. 9). This is a useful method to orient the exchange bias field in different directions in different magnetic layers in more complicated magnetic structures. By using AF layers with different blocking temperatures different, F layers can thereby be exchange biased in different directions. This is useful for engineering magnetic structures for various applications. A variety of models have been proposed to account for an exchange bias field even in the presence of rough interfaces (Malozemoff, 1988; Koon, 1997).

By combining an exchange biased ferromagnetic layer with a simple ferromagnetic layer it is thereby possible to engineer the magnetic moments of the two layers to be either parallel or antiparallel to one another as a function of magnetic field without relying on interlayer exchange coupling. Examples of such spin-valve GMR sandwiches are shown in Fig. 10 (Parkin, 1993). In each case a thin Co or permalloy layer, *pinned* by exchange biasing to a thin MnFe antiferromagnetic layer, is separated from an unpinned or *free* thin Co or permalloy layer by Cu layers $\sim 20 \text{ \AA}$ thick. The interlayer coupling via the Cu layer is weak. As shown in Fig. 10, well defined magnetic states of the sandwich are obtained in small positive and negative fields with the magnetic moments of the pinned and free layers parallel or anti-parallel to one another. This leads, via the GMR effect, to a step-wise change

An antiferromagnet grown in the absence of a magnetic field has no long-range magnetic order



A disordered antiferromagnet layer adjacent to a hard ferromagnetic layer may be magnetically ordered by heating above its blocking temperature and subsequently cooling

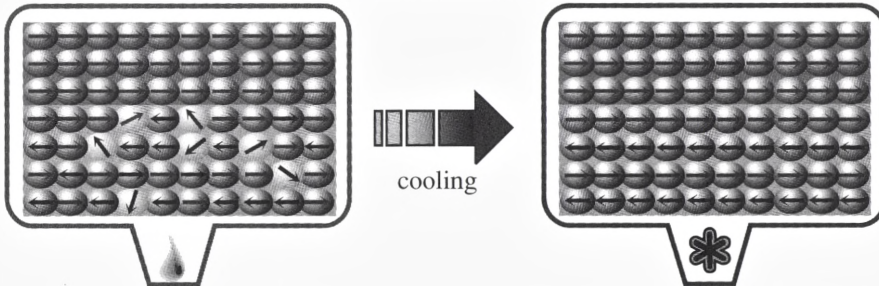


Figure 9. Schematic depiction of exchange biasing of a ferromagnetic layer by an antiferromagnetic layer.

in the resistance of the sandwich in small magnetic fields. The magnitude of the GMR effect in such sandwiches is very small, 3–7%, as compared with more than 100% in the Co–Fe/Cu multilayer shown in Fig. 3. A great deal of the GMR effect has been sacrificed to engineer a structure useful for MR head applications. The magnitude of the GMR in the sandwich is reduced for various reasons, including that there are only two magnetic layers (Parkin, 1995), and that the Cu spacer layer and the magnetic layers themselves are relatively thick leading to increased dilution of the GMR effect (Parkin et al., 1993). By using additional magnetic layers such that the free FM layer has two pinned magnetic layers on either side of it, GMR values of more than 20% have been obtained at room temperature (Egelhoff et al., 1995).

The origin of the GMR effect has been much debated since its discovery a few years ago (Binasch et al., 1989; Baibich et al., 1988). Much discussion has related to the role of spin-dependent scattering of the conduction electrons at the interfaces between the F and spacer layers. Early models emphasized the role of spin-dependent scattering within the interior of the F layers (Camley and Barnas, 1989; Levy, 1994) but subsequent work has revealed that the interfacial scattering

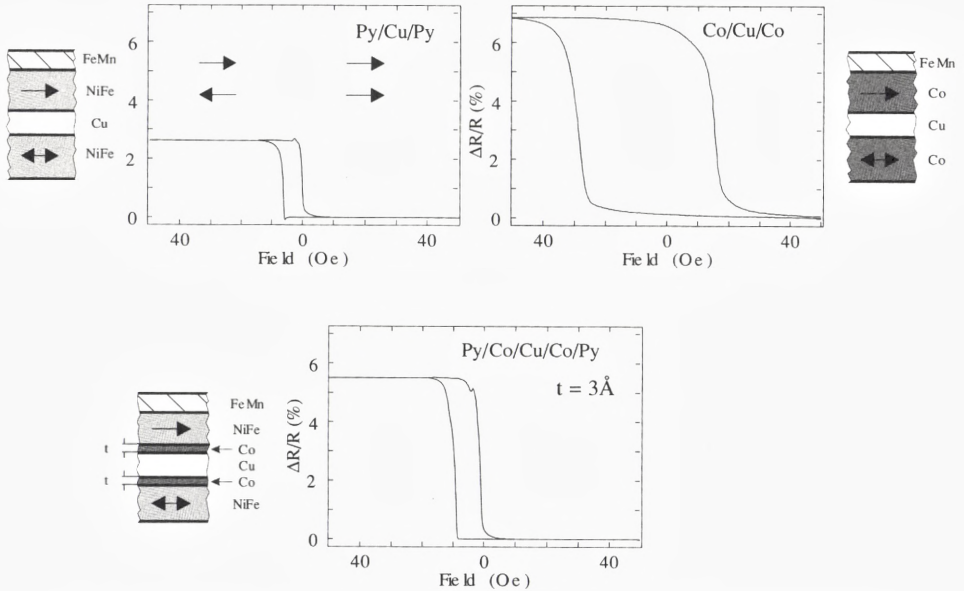


Figure 10. Resistance versus field curves for three spin-valve GMR exchange-biased structures: Py/Cu/Py, Co/Cu/Co and a Py/Cu/Py sandwich with 3 Å Co interface layers. (Py=permalloy).

is the dominant contribution (Parkin, 1992, Parkin, 1993). This is clearly demonstrated in Fig. 10 in which room temperature resistance versus field curves are shown for three spin-valve sandwiches. Fig. 10(a) shows data for Si/ 53Å Py/ 32Å Cu/ 22Å Py / 90Å FeMn/ 10Å Cu, where Py is permalloy ($\text{Ni}_{81}\text{Fe}_{19}$). The Py free layer in the Py/Cu/Py sandwich exhibits a very small switching field so that the structure is very sensitive to small fields. Data for a similar structure with the Py layers replaced by Co is shown in Fig. 10(b). The MR of the sandwich with Co layers is about twice as large as that of the Py/Cu/Py structure. However the Co free layer displays a significantly higher switching field than Py since Co has a much higher anisotropy. By simply dusting each of the Py/Cu interfaces in structure (a) with very thin layers of Co a structure with MR comparable to that of the Co/Cu structure but with low switching fields corresponding to the Py/Cu structure is obtained. Data for a sandwich with the same structure as in (a) but with 3 Å thick Co layers added at each Py /Cu interface is shown in Fig. 10 (c). Only 1–2 atomic layers of Co, just sufficient to completely cover the Py/Cu interface is required to obtain the enhanced GMR of the Co/Cu structure (see Fig. 11) (Parkin, 1993).

Finally another example of the dominant role of interface scattering in magnetic

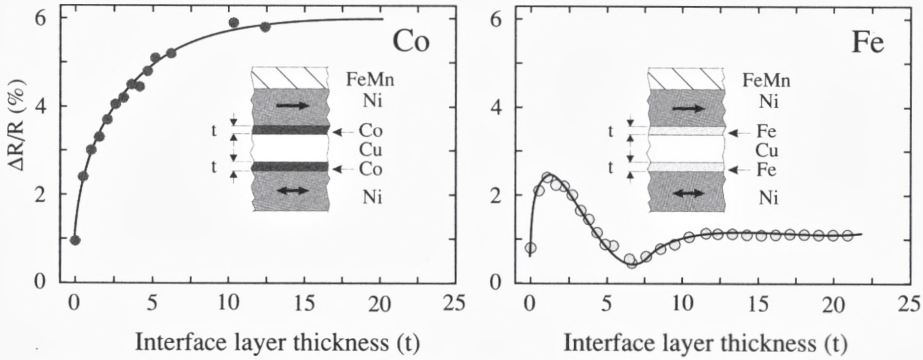


Figure 11. Saturation magnetoresistance versus thickness of Co and Fe layers inserted at the Ni/Cu interfaces in an exchange biased Ni/Cu/Ni spin valve GMR structure.

multilayers is shown in Fig. 11. The figure shows the results of dusting the Ni/Cu interfaces in Ni/Cu/Ni exchange biased sandwiches with Co and Fe. For Co interface layers the MR systematically increases as the Co interface layer is thickened, increasing by about a factor of six for Co layers about 10 Å thick. By contrast the MR of Ni/Cu/Ni structures has a complicated dependence on the thickness of Fe interface layers. The MR initially increases with the insertion of 1–2 Å Fe, then decreases and finally increases with thicker Fe layers. The dependence of the MR on Fe thickness can be accounted for by changes in the crystal structure, and consequently the magnetic moment of the Fe layer. For very thin Fe layers the Fe takes up a tetragonally distorted fcc phase which is ferromagnetic. For intermediate Fe thicknesses the Fe takes up an undistorted fcc phase which has no net magnetic moment and, finally, for thicker Fe layers, the Fe structure changes to a bcc phase which again is ferromagnetic. Details of the structure and magnetism of the Fe layers has been explored in related sputter-deposited crystalline (100) Ni/Fe superlattices (Kuch and Parkin, 1997).

5 Summary

Transition metal magnetic multilayers display fascinating properties. These include the indirect magnetic exchange coupling of thin 3d ferromagnetic layers of Co, Fe, Ni and their various alloys via intervening spacer layers of almost any of the non-ferromagnetic transition or noble metals. The indirect coupling is long-range and oscillates between ferro- and antiferromagnetic coupling as the spacer layer thickness is varied. Antiferromagnetically coupled multilayers display enhanced

magnetoresistance values. These giant magnetoresistance values have magnitudes of as much as $\sim 110\%$ and $\sim 220\%$ at room temperature and helium temperatures, respectively. The oscillatory interlayer coupling makes possible the *spin* engineering of magnetic multilayers with all sorts of possible magnetic structures (Parkin and Mauri, 1991). Simple sandwich structures composed of two ferromagnetic layers separated by thin Cu layers can be optimized, using interfacial dusting, to give large changes in resistance in very small magnetic fields. Such structures show great potential for magnetic recording read head sensors.

Acknowledgements

I thank Arley Marley and Kevin Roche (IBM Almaden Research Center), Tom Rabedeau (Stanford Synchrotron Radiation Laboratory) and David Smith (Arizona State University) for their important contributions to parts of the work discussed here. I also thank Robin Farrow and Mike Toney for many useful discussions.

References

- Almeida NS and Mills DL, 1995: Phys. Rev. B **52**, 13504
Azevedo A, Chesman C, Rezende SM, Aguiar FMD, Bian X and Parkin SSP, 1996: Phys. Rev. Lett. **76**, 4837
Baibich MN, Broto JM, Fert A, Dau FNV, Petroff F, Etienne P, Creuzet G, Friederich A and Chazelas J, 1988: Phys. Rev. Lett. **61**, 2472
Binasch G, Grünberg P, Saurenbach F and Zinn W, 1989: Phys. Rev. B **39**, 4828
Bruno P and Chappert C, 1992: Phys. Rev. B, **46**, 261
Camley RE and Barnas J, 1989: Phys. Rev. Lett. **63**, 664
Cebollada A, Martinez JL, Gallego JM, Miguel JJD, Miranda R, Ferrer S, Batallan F, Fillion G and Rebouillat JP, 1989: Phys. Rev. B **39**, 9726
Chien CL, 1995: in Annu. Rev. Mater. Sci., ed. B.W. Wessels (Annual Reviews Inc., Palo Alto) Vol. 25, p. 129–160
Ciureanu P, 1992: in *Thin Film Resistive Sensors*, eds. P. Ciureanu and S. Middelhoek (Institute of Physics Publishing, Bristol)
Dieny B, Gavigan JP and Rebouillat JP, 1990: J. Phys. Condens. Matter **2**, 159
Dieny B, Speriosu VS, Parkin SSP, Gurney BA, Wilhoit DR and Mauri D, 1991: Phys. Rev. B **43**, 1297
Egelhoff WF, Ha T, Misra RDK, Kadmon Y, Nir J, Powell CJ, Stiles MD, Michael RD, Lin CL, Silvertsen JM, Judy JH, Takano K, Berkowitz AE, Anthony TC and Brug JA, 1995: J. Appl. Phys. **78**, 273
Farrow RFC, Harp GR, Marks RF, Rabedeau TA, Toney MF, Weller D and Parkin SSP, 1993: J. Cryst. Growth **133**, 47
Fert A and Bruno P, 1994: in *Ultrathin Magnetic Structures*, eds. B. Heinrich and J.A.C. Bland (Springer-Verlag, Berlin) Vol. II, p. 82
Folkerts W, 1991: J. Magn. Magn. Mater. **94**, 302
Fujiwara H, 1995: IEEE Trans. Magn. **31**, 4112

- Fulghum DB and Camley RE, 1995: Phys. Rev. B **52**, 13436
- Fullerton EE, Conover MJ, Mattson JE, Sowers CH and Bader SD, 1993: Phys. Rev. B **48** 15755
- Fullerton EE, Riggs KT, Sowers CH, Berger SD and Berger A, 1995: Phys. Rev. Lett. **75**, 330
- Grochowski E and Thompson DA, 1994: IEEE Trans. Magn. **30**, 3797
- Harp GR and Parkin SSP, 1994: Appl. Phys. Lett. **65**, 3063
- Harp GR and Parkin SSP, 1996: Thin Solid Films **288**, 315
- Johnson MT, Coehoorn R, Vries JJD, McGee NWE, Stegge JAD and Bloemen PJH, 1992: Phys. Rev. Lett. **69**, 969
- Koon NC, 1997: (preprint)
- Kuch W and Parkin SSP, 1997: Europhys. Lett. **37**, 465
- Lenczowski SKJ, Gijs MAM, Giesbers JB, van de Veerdonk RJM and Jonge WJM, 1994: Phys. Rev. B **50**, 9982
- Levy PM, 1994: in *Solid State Physics*, eds. H. Ehrenreich and D. Turnbull (Academic Press, New York) Vol. 47, p. 367
- Lurio LB, Rabedeau TA, Pershan PS, Silvera IF, Deutsch M, Kosowsky SD and Ocko BM, 1992: Phys. Rev. Lett. **68**, 2628
- Malozemoff AP, 1988: J. Appl. Phys. **63** 3874
- Mathon J, Villeret M, Muniz RB, Castro JDAE and Edwards DM, 1995: Phys. Rev. Lett. **74**, 3696
- McGuire TR and Potter RI, 1975: IEEE Trans. Magn. **MAG-11**, 1018
- Parkin SSP, 1991: Phys. Rev. Lett. **67**, 3598
- Parkin SSP, 1992: Appl. Phys. Lett. **61**, 1358
- Parkin SSP, 1993: Phys. Rev. Lett. **71**, 1641
- Parkin SSP, 1994: in *Ultrathin Magnetic Structures*, eds. B. Heinrich and J.A.C. Bland (Springer-Verlag, Berlin) Vol. II, p. 148
- Parkin SSP, 1995: in *Annual Review of Materials Science*, ed. B.W. Wessels (Annual Reviews Inc., Palo Alto) Vol. 25, p. 357-388
- Parkin SSP, Bhadra R and Roche KP, 1991a: Phys. Rev. Lett. **66**, 2152
- Parkin SSP, Li ZG and Smith DJ, 1991b: Appl. Phys. Lett. **58**, 2710
- Parkin SSP, Mansour A and Felcher GP, 1991c: Appl. Phys. Lett. **58**, 1473
- Parkin SSP and Mauri D, 1991: Phys. Rev. B **44**, 7131
- Parkin SSP, Modak A and Smith DJ, 1993: Phys. Rev. B **47**, 9136
- Parkin SSP, More N and Roche KP, 1990: Phys. Rev. Lett. **64**, 2304
- Parratt LG, 1954: Phys. Rev. B **95**, 359
- Pettit K, Gider S, Salamon MB and Parkin SSP 1997: (preprint)
- Pierce DT, Unguris J and Celotta RJ, 1994: in *Ultrathin Magnetic Structures*, eds. B. Heinrich and J.A.C. Bland (Springer-Verlag, Berlin) Vol. II
- Rossiter PL, 1987: *The electrical resistivity of metals and alloys* (CUP, Cambridge)
- Rührig M, Schäfer R, Hubert A, Mosler R, Wolf JA, Demokritov S and Grünberg P, 1991: Phys. Status Solidi A **125**, 635
- Sinha SK, Sanyal MK, Gibaud A, Satija SK, Majkrzak CF and Homma H, 1991: in *Science and Technology of Nanostructured Magnetic Materials*, eds. G.C. Hadjipanayis G.A. and Prinz (Plenum Press, New York) Vol. B259, p. 145
- Slonczewski JC, 1995: J. Magn. Magn. Mater. **150**, 13
- Smith DJ, Li ZG, Modak AR, Parkin SSP, Farrow RFC and Marks RF, 1994: Scr. Metall. Mater. **30**, 689
- Smith DJ, Modak AR, Rabedeau TA and Parkin SSP, 1997: (submitted)
- Toney MF and Thompson C, 1990: J. Chem. Phys. **92**, 3781
- Tsang C, Chin MM, Togi T and Ju K, 1990: IEEE Trans. Magn. **26**, 1689
- Unguris J, Celotta RJ and Pierce DT, 1991: Phys. Rev. Lett. **67** 140

Weber W, 1995: *Europhys. Lett.* **31** 491

Yelon A, 1971: in *Physics of Thin Films: Advances in Research and Development*, eds. M. Francombe and R. Hoffman (Academic Press, New York) Vol. 6, p. 205